

# Micromachined flow-through filter-chamber for chemical reactions on beads

Helene Andersson\*, Wouter van der Wijngaart, Peter Enoksson, Göran Stemme

*Instrumentation Laboratory, Royal Institute of Technology, 100 44 Stockholm, Sweden*

Accepted 20 March 2000

## Abstract

A new flow-through micromachined device for chemical reactions on beads has been designed, manufactured, and characterized. The device has an uncomplicated planar design and microfabrication process. Both nonmagnetic and magnetic beads can be collected in the reaction chamber without the use of external magnets. The sample flow-through volume of liquid or gas is adjustable and unlimited. The device is sealed with Pyrex to allow real time optical detection of the chemical reactions. At a constant pressure of 3 kPa at the inlet the flow rate for water is about 3.5  $\mu\text{l}/\text{min}$  without beads in the filter chamber, for all the designs. The smallest reaction chamber has a volume of 0.5 nl and can collect approximately 50 beads with a diameter of 5.50  $\mu\text{m}$ . At a constant pressure of 3 kPa at the inlet, the flow rate for water is about 2.0  $\mu\text{l}/\text{min}$  when the reaction chamber is completely packed with beads. Hence, the flow rate decreases with about 40% when the reaction chamber is packed with beads. The flow-through microfluidic device is not sensitive to gas bubbles, and clogging of the filter is rare and reversible. The beads are easy to remove from the reaction chamber making the micromachined flow-through device reusable. A new and simple technique for fluid interconnection is developed. © 2000 Elsevier Science B.V. All rights reserved.

*Keywords:* Bead trapping; Bead handling; Microfluidics; Micro total analysis system

## 1. Introduction

Microfluidic devices for manipulating microspheres have, until today, mainly involved magnetic microspheres and have primarily focused on magnetically activated separations [1].

Microspheres, also known as beads, are routinely used as the mobile solid phase in medical diagnostics, microbiology, cancer research, immunology and molecular biology for separation, synthesis and detection of molecules. The uniformity of the beads and their precisely defined size ensure that each bead has identical chemical and physical properties. Beads are available in several different materials and sizes (a few nanometers to millimeters in diameter). The surface chemistry of the beads can be modified with various functional groups rendering the beads hydrophobic, hydrophilic, fluorescent, or active towards special ligand binding proteins.

In order to perform and detect chemical reactions on beads, they must be confined to a limited volume. Paramagnetic beads, i.e. beads with a magnetite ( $\text{Fe}_3\text{O}_4$ ) core sealed in a polymer shell, are extensively used today because they can be conveniently separated by applying external magnets [2]. However, magnetic principles are not always advantageous in micro total analysis systems ( $\mu\text{-TAS}$ ) applications. External magnetic systems complicate precision handling and result in a bulky system. Incorporation of magnetic components on wafer level is also a very complicated process [3].

To perform chemical reactions on nonmagnetic and magnetic beads, a flow-through microfluidic device for bead trapping has been designed, manufactured, and characterized.

The device has an uncomplicated design and is batch fabricated by deep reactive ion etching (DRIE). It is sealed by anodically bonded Pyrex to enable real time optical detection.

Although a wide range of different  $\mu\text{-TAS}$  has been demonstrated [4], efficient standard interconnections between these devices and the macroscopic world are not yet

\* Corresponding author. Tel.: +46-8-790-92-36; fax: +46-8-10-08-58.  
E-mail address: helene.andersson@s3.kth.se (H. Andersson)

available [5]. Therefore, a new and simple melt-on method for conveniently fixing external tubes to the chip was developed.

The great assortment of available beads and the characteristics of the device presented in this paper open up the possibility to miniaturize many experiments that are today performed in test tubes or microtiter plates. In addition, the flow-through microfluidic reaction chamber may have a potential role in applications not involving beads, i.e. cell–cell separations, cell deformability tests and particle filtration [6,7].

## 2. Design

A simple design for a particle trapping component in a flow-through device consists of a grid of small pillars. The variable number of pillars, composing the filter, can have different shapes and pitch. The geometrical placement of the pillars is constrained by three demands. Firstly, the flow resistance of the filter must remain within certain limits. Secondly, the filter should not be sensitive to clogging. Finally, the collected beads should be held within a relatively small confined area to facilitate detection. Some basic micro filter designs are presented in Fig. 1.

In Fig. 1(a) the filter is placed inside a flow channel. The number of pillars is limited by the channel width. For a narrow channel ( $50\ \mu\text{m}$ ) this means a small number of pillars (20) resulting in a high sensitivity for clogging (design 9 in this study). In Fig. 1(b) the channel is widened at the entrapment location. This design diminishes the risk for clogging and results in homogeneous flow character-

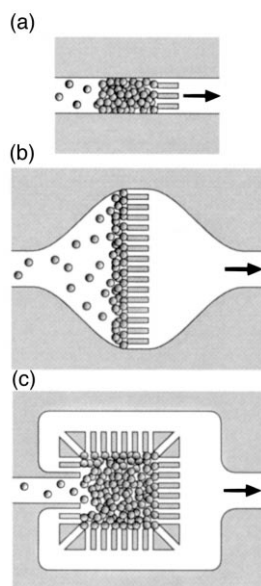


Fig. 1. Different micro filter designs. (a) The filter pillars are placed inside the channel. (b) The channel is widened at the bead trapping location. (c) The filter pillars define a square reaction chamber where the beads are collected.

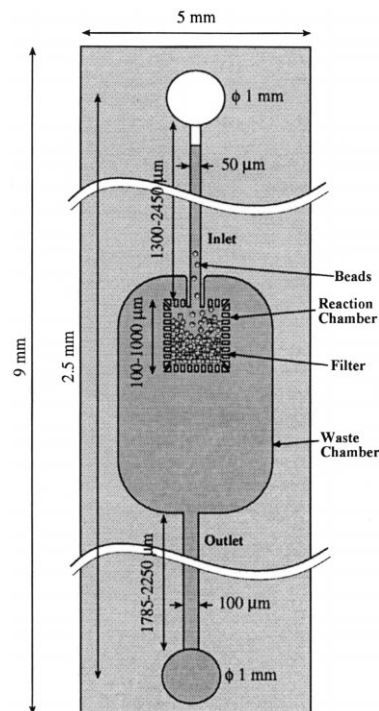


Fig. 2. A schematic of the micromachined flow-through device.

istics over the filter. One drawback for the detection is that the beads are confined to a long strip instead of a small square or round area. The design in Fig. 1(c) does not suffer from this restriction. The pillars define a square reaction chamber in which the beads are trapped. A larger number of pillars (70–790) constitute the filter, which results in a less clogging sensitive filter. The design in Fig. 1(c) fulfils the design criteria mentioned above and was therefore chosen for fabrication and evaluation.

A schematic of the complete flow-through microfluidic device is shown in Fig. 2. The beads are applied at the inlet and collected in the reaction chamber. The waste chamber is surrounding the reaction chamber and connected to the outlet.

The sample flow-through does not displace the beads or their surface functional groups and multi-step reactions can be implemented at one location in the microfabricated device. Several different designs were included in the study to evaluate the bead capture efficiency, mechanical strength of the pillars, and fluid dynamics of the reaction chamber. In addition, a comparison was made between a micromachined filter in a channel (Fig. 1(a)) and the designs presented here (Fig. 1(c)).

## 3. Fabrication

The flow-through device was manufactured using standard photolithographic procedures and bulk micromachining of silicon. The two-level-mask fabrication process involves a limited number of techniques, i.e. DRIE and

anodic bonding. Hundred millimeter in diameter 525  $\mu\text{m}$  thick p-doped silicon (100)-wafers were used as starting material. Photoresist (1.5  $\mu\text{m}$  thick) constitutes both etch masks. First, the front side was patterned and etched using DRIE (Surface Technology Systems, UK) defining the inlet channel, reaction chamber, filter, waste chamber and outlet channel. To seal the device, a 170, 300 or 500  $\mu\text{m}$  thick Pyrex glass wafer was anodically bonded to the front side. The backside was then patterned and a second DRIE step creates fluid connections. The silicon–glass stack was sawed into  $9 \times 5$  mm chips.

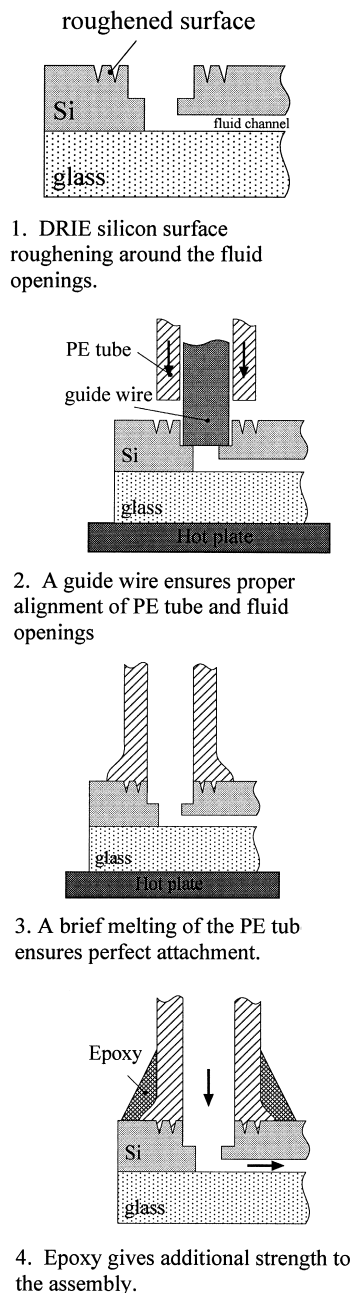


Fig. 3. Attachment of the fluid connectors by using a new melt-on method.

External polyethylene (PE) tubes were used as fluid connectors and were fixed to the chip in a multi-step procedure as schematically shown in Fig. 3. A mask-defined silicon surface roughening was performed around the fluid openings by the second DRIE to ensure good adhesion of the PE tubes. A guide wire was used to align the PE tube with the fluid openings on the chip during the tube fixing process. The silicon–glass stack was shortly heated to generate a local melting of the PE tube onto the chip. To give additional strength to the assembly, the interface between the chip and the PE tubes was covered with epoxy glue.

#### 4. Experimental

The dimensions of the micromachined structures were measured using a scanning electron microscope and compared with the original specifications. The consistency of the filter pillar dimensions within a reaction chamber and between different reaction chambers was measured.

The fluid behaviour of the flow-through micromachined device was first investigated for water without beads. A constant pressure of 3 kPa was applied at the inlet and the flow rate was determined by measuring the speed of the liquid column. To test the ability of the reaction chamber to collect beads and concurrently enable unlimited flow-through, streptavidin coated beads of two different materials and sizes were used, i.e. polystyrene beads with a diameter of 5.50  $\mu\text{m}$  (Bangs Laboratories, IN, USA) and magnetic Dynabeads with a diameter of 2.8  $\mu\text{m}$  (Dyna, Norway). The bead solutions were applied manually with a pipette under a standard light microscope with  $40\times$  objective. To enable detailed observations of individual beads in the microfluidic device, the beads were applied at a low concentration (10 000 beads/ml). Samples at the outlet were collected and controlled under the microscope to confirm that beads do not pass through the filter.

#### 5. Results

Table 1 presents the different design parameters of the filter-chamber for chemical reactions on beads. Design 9 is a channel with a filter inside (see Fig. 1(a)), which is used for comparison with the new designs (see Fig. 1(c)).

Fig. 4 shows a scanning electron microscope (SEM) photo of the new microfluidic device (design 1) for bead trapping defining inlet channel, reaction chamber, filter pillars, waste chamber and outlet channel. The respective scale bar appears at the bottom of all the SEM figures. A higher magnification of the reaction chamber is shown in Fig. 5 in a top (a) and side (b) view, while Fig. 6 shows the filter pillars in detail. The scalloped pattern is a result of the gas switching in the DRIE process.

Table 1

A summary of the different designs of the flow-through micromachined device where  $V$  is the filter chamber volume,  $W$  the pillar width,  $L$  the pillar length, and  $H$  the pillar height

Design	Reaction chamber $V$ (nl)	Pillar $W$ , $L$ , $H$ ( $\mu\text{m}$ )	Pillar spacing ( $\mu\text{m}$ )	Number of pillars	Inlet channel $W$ , $L$ , $H$ ( $\mu\text{m}$ )	Outlet channel $W$ , $L$ , $H$ ( $\mu\text{m}$ )
1	0.5	3, 10, 50	2	70	50, 2450, 50	100, 2250, 50
2	2.0	3, 10, 50	2	152	50, 2450, 50	100, 2000, 50
3	12.5	3, 10, 50	2	392	50, 2250, 50	100, 1785, 50
4	50.0	3, 10, 50	2	792	50, 1300, 50	100, 1480, 50
5	0.5	3, 5, 50	2	70	50, 2450, 50	100, 2250, 50
6	0.5	3, 20, 50	2	70	50, 2450, 50	100, 2250, 50
7	12.5	3, 10, 50	3	320	50, 1300, 50	100, 1785, 50
8	12.5	5, 10, 50	4	220	50, 1300, 50	100, 1785, 50
9	10	3, 10, 50	2	20	50, 2285, 50	100, 2225, 50

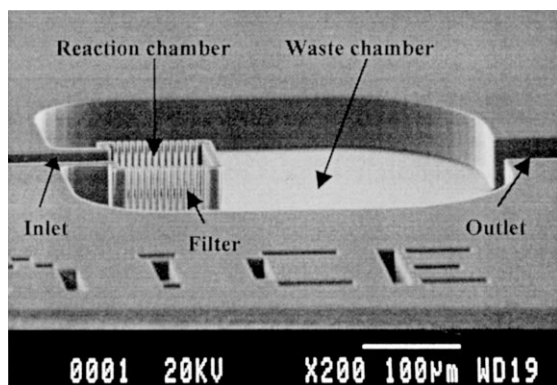


Fig. 4. A SEM overview of the flow-through micromachined device (design 1).

The dimensions of the measured structures are in good agreement with the original specifications. The micromachined structures are found to have high uniformity indicating a uniform and reproducible fabrication process.

The melt-on method for fixing the external PE tubes to the chip was found to be very convenient and reliable. It results in robust, precisely positioned interconnections to

the macroscopic world with low dead volumes. It is mainly the epoxy glue which gives the assembly the robustness.

To investigate the fluid behaviour of the microfluidic device, water without beads was first applied. The flow rate for water was about  $3.5 \mu\text{l}/\text{min}$  for all the designs presented in Table 1 when a constant pressure of 3.0 kPa was applied at the inlet. The different filter dimensions and number of pillars proved to have no significant influence on the pressure drop for water.

The reaction chamber was easily packed with beads while observed through the microscope. The beads pass freely through the inlet channel and pack the reaction chamber from bottom to top. All designs successfully capture beads with a diameter of  $5.50 \mu\text{m}$ . No beads were observed to pass through the filter, hence no beads were found in the filtered liquid at the outlet when controlled under the microscope.

The smallest reaction chamber (design 1, 5, 6) has a volume of 0.5 nl and can hold about 50 beads with a diameter of  $5.50 \mu\text{m}$ . There is no upper limitation of the flow-through volume of liquid or gas, which is important when working with very low sample concentrations. The smallest volume required to fill the device is 3.0 nl (the volume of the inlet channel and reaction chamber).

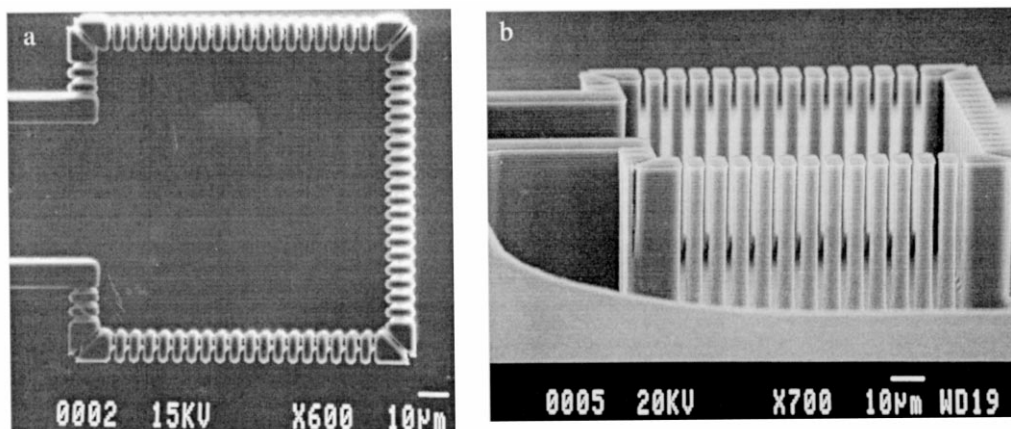


Fig. 5. SEM images of the reaction chamber (design 1) in top (a) and side (b) view.

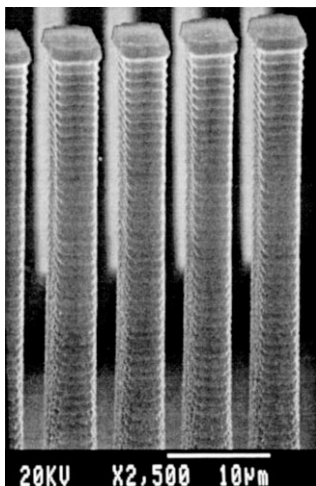


Fig. 6. A high magnification of the pillars constituting the filter in the reaction chamber (design 1). The scalloped pattern is a result of the gas switching in the DRIE process.

The flow rate for water was about 2.2  $\mu\text{l}/\text{min}$  (when a constant pressure of 3.0 kPa was applied at the inlet) for all the designs when the reaction chamber is completely packed with beads. Hence, the flow rate decreases with about 40% when the reaction chamber is packed with beads. The different dimensions of the reaction chamber and number of pillars did not affect the flow rate significantly.

Analytical calculations were performed to verify the pressure drop over the different components, i.e. the inlet and outlet channel, and the filter in the reaction chamber without beads. Poiseuille's law was used for calculating the pressure drop over the channels [8]. The pressure drop over the filter was calculated as for a number of parallel short channels using

$$\Delta P = Q_v C \mu / 2 A D_h^2 \quad (1)$$

where  $\Delta P$  is the pressure drop,  $Q_v$  the volumetric flow,  $C$  the friction coefficient (96 for rectangular cross-section  $w \gg h$ ),  $\mu$  the fluid dynamic viscosity,  $A$  the cross-sectional area of flow path and  $D_h$  the hydraulic diameter [9]. Eq. (1) is valid when  $2 < L/D_h < 50$  where  $L$  is the

length of the channel [8]. In Table 2 the calculated pressure drop for the in- and outlet channel and the filter at a flow rate of 3.5  $\mu\text{l}/\text{min}$  is presented. For comparison, the applied pressure to achieve the same flow rate (3.5  $\mu\text{l}/\text{min}$ ) is included in Table 2. The theoretic and experimental results are in very good agreement. It can be seen that the main pressure drop is across the inlet and outlet channels even for the smallest filter design.

Clogging of the filters is rare and can easily be removed by applying back-pressure. It was concluded that designs 1–8 are much less sensitive to clogging than design 9. This is probably due to the larger filter area present in designs 1–8. Design 9 is a channel with only 20 pillars constituting the filter compared to 70–790 pillars for design 1–8.

Selectivity tests were performed on design 7 and 8 using a mixture of 2.8  $\mu\text{m}$  and 5.50  $\mu\text{m}$  beads. The larger beads were efficiently captured in the reaction chamber while the smaller beads easily passed through the filter.

Gas bubbles present in the samples did not affect the device performance. The beads can easily be removed out of the reaction chamber by applying back-pressure. After removing the beads and carefully cleaning of the micromachined flow-through device, it can be reused.

## 6. Discussion

The flow-through micromachined reaction chamber presented here collects both nonmagnetic and magnetic beads. Nonmagnetic beads have lower density resulting in improved fluid dynamic behaviour in  $\mu\text{-TAS}$  compared to magnetic beads.

The batch fabrication process of the flow-through microfluidic device is simple and reproducible, involving only two masks and two different processing techniques. These are important factors in terms of parallelization and producing cost effective economical  $\mu\text{-TAS}$ . The chip dimensions ( $9 \times 5$  mm) were chosen to simplify practical handling and can be further reduced if required. The smallest reaction chamber of 0.5 nl, collecting approximate 50 beads, can also be further miniaturized if a reduced number of beads or flow-through volume are of interest.

Table 2

Calculated and applied pressure drop (at the inlet) for a constant flow rate of 3.5  $\mu\text{l}/\text{min}$

Design	Calculated pressure drop across the inlet (kPa)	Calculated pressure drop across the outlet (kPa)	Calculated pressure drop across the filter (kPa)	Calculated total pressure drop (inlet, outlet and filter) (kPa)	Applied pressure (kPa) to obtain a flow rate of 3.5 $\mu\text{l}/\text{min}$	Calculated vs. applied pressure drop (%)
1	1.7	0.5	0.3	2.5	3	83
2	1.7	0.4	0.1	2.2	3	73
3	1.6	0.4	0.04	2.0	3	67
4	0.9	0.3	0.02	1.2	3	40
5	1.7	0.5	0.1	2.3	3	77
6	1.7	0.5	0.5	2.7	3	90
7	1.6	0.4	0.02	2.0	3	67
8	1.6	0.4	0.01	2.0	3	67
9	1.6	0.5	0.9	3.0	3	100

To seal the device, different thicknesses (170–500  $\mu\text{m}$ ) of Pyrex were used to enable real time optical detection of the chemical reactions on the beads in the reaction chamber. The thinnest Pyrex wafer will be used for detection of chemical reaction generating only a few photons. Since the sample flow-through does not displace the beads or their surface functional groups multi-step reactions can be implemented at one location in the microfabricated device, facilitating optical detection.

The sample flow-through rate is adjustable, which is important when performing chemical reactions on beads [10]. Unlimited flow-through volumes of gas and liquid are realized allowing detection of rare molecules or biological species (at or below 100 copies/ml) [11]. The flow-through microfluidic reaction chamber reduces the accumulation of by-products resulting in increased reaction and detection sensitivity compared to a closed system (i.e. microtiter plates).

The different designs of the reaction chamber included in the study do not significantly affect the device performance (i.e., bead capture, air bubble sensitivity, pressure drop) for bead assays as long as the pillars constitute a mechanical barrier. Analytical calculations showed that the largest pressure drop is located across the inlet and outlet channels. The reaction chamber and filter dimensions can therefore be optimized for bead size and chemical reaction parameters. For cell-based assays, the filter dimensions are important. For example, when filtering cells it is important that the cells pass through the filter as quickly as possible to reduce cell activation, stiction and cell rupture [12].

For performing chemical reactions on the beads in the microfluidic device, it is important that the flow resistance remains low when the reaction chamber is packed with beads. Otherwise, it is difficult to pump the reactants through the reaction chamber. For the devices presented here, the flow rate decreases with 40% when the reaction chamber is packed with beads. This corresponds to a flow of about 2  $\mu\text{l}/\text{min}$ , which is still well within the margins for  $\mu\text{-TAS}$ .

Future developments include solid-phase DNA sequencing, automatic introduction of beads by using micropumps, parallelization and device fabrication using plastic replication techniques.

## References

- [1] P. Telleman, U. Larsen, J. Philip, G. Blankenstein, A. Wolff, Cell sorting in microfluidic systems, in: Micro Total Analysis Systems '98, Banff Canada, Oct 13–16, 1998, pp. 39–44.
- [2] O. Olsvik, T. Popovic, E. Skjerve, K.S. Cudjoe, E. Hornes, J. Ugelstad, M. Uhlen, Magnetic separation techniques in diagnostic microbiology, *Clin. Microbiol. Rev.* 7 (1994) 43–54.
- [3] C. Ahn, M. Allen, W. Trimmer, Y. Jun, S. Erramilli, A fully integrated micromachined magnetic particle separator, *J. Microelectromech. Syst.* 5 (1996) 151–158.
- [4] A. van der Berg, T. Lammerink, Micro total analysis systems: microfluidic aspects, integration concept and applications, *Top. Curr. Chem.* 194 (1998) 21–49.
- [5] D. Jaeggi, R. Gray, N. Mourlas, R. Drienhuizen, Novel interconnection technologies for integrated microfluidic systems, in: Solid State Sensor and Actuator Workshop, Hilton Head Island, South Carolina, June 8–11, 1998, pp. 112–115.
- [6] L. Christel, K. Petersen, W. McMillian, M. Northrup, Rapid, automated nucleic acid probe assays using silicon microstructures for nucleic acid concentration, *J. Biomech. Eng.* 121 (1997) 22–27.
- [7] R. Carlson, C. Gabel, S. Chan, R. Austin, Self-sorting of white blood cells in a lattice, *Phys. Rev. Lett.* 79 (1997) 2149–2152.
- [8] F. White, *Fluid mechanics*, 2nd edn., McGraw-Hill, New York, 1986.
- [9] P. Gravens, J. Branbjerg, O. Sondergard Jensen, *Microfluidics — a review*, *J. Micromech. Microeng.* 5 (1993) 168–182.
- [10] S. Ostergaard, G. Blankenstein, H. Dirac, O. Leistiko, Reagent handling by manipulation of magnetic particles: A new approach to the automation and miniaturisation of analytical chemistry, in: Micro Total Analysis Systems '98, Banff Canada, Oct 13–16, 1998, pp. 411–414.
- [11] A. Manz, N. Graber, M. Widmer, Miniaturized total chemical analysis systems: a novel concept for chemical sensing, *Sens. Actuators B* 1 (1990) 244–248.
- [12] C. van Rijn, W. Nijdam, M. Elwenspoek, A microsieve for leukocyte depletion of erythrocyte concentrates, in: 18th Annual International Conference of the IEEE Engineering in Medicine and Biology Society, Amsterdam, 1997, pp. 256–257.

## Biographies

*Helene Andersson* was born 1974 in Hudiksvall, Sweden. She received her MSc degree in Molecular Biotechnology in 1998 from Uppsala University, Sweden. In the beginning of 1999 she started her PhD studies at the department of Signals, Sensors and Systems at the Royal Institute of Technology, Stockholm, Sweden. Her main research areas are microfluidics, micro total analysis systems, micropumps and nanochemistry.

*Wouter van der Wijngaert* was born 1973 in Lokeren, Belgium. He received his MSc in Electrotechnical Engineering in 1996 at the University of Leuven, Belgium. He is currently working on his PhD studies at the department of Signals, Sensors and Systems at the Royal Institute of Technology, Stockholm, Sweden. His main research areas are microfluidics and microfluidic actuators.

*Peter Enoksson* was born in Lindesberg, Sweden, on April 19, 1957. He received the MSc degree in Engineering Physics in 1986, the Licentiate of Engineering in 1995 and the PhD in 1997 all from the Royal Institute of Technology, Stockholm, Sweden. In 1997 he was appointed Assistant Professor at the silicon sensor research group at the Department of Signals, Sensors and Systems at the Royal Institute of Technology. His research is in the field of resonant silicon sensors and actuators, especially for fluid applications.

*Göran Stemme* was born in Stockholm, Sweden, on February 4, 1958. He received the MSc degree in electrical engineering in 1981 and the PhD degree in solid state electronics in 1987, both from the Chalmers University of Technology, Gothenburg, Sweden. In 1981, he joined the Department of Solid State Electronics, Chalmers University of Technology, Gothenburg, Sweden. There, in 1990, he became an Associate Professor (Docent) heading the silicon sensor research group. In 1991, Dr. Stemme was appointed Professor at The Royal Institute of Technology, Stockholm, Sweden. He heads the Instrumentation Laboratory at the department of Signals, Sensors and Systems. His research is devoted to sensors and actuators based on micromachining of silicon. Dr. Stemme is a Subject Editor for the IEEE/ASME Journal of Microelectromechanical Systems.